



First observation of the charge carrier density related gain reduction mechanism in LGADs with the Two Photon Absorption-Transient Current Technique

S. Pape ^{a,b,*}, E. Currás ^a, M. Fernández García ^c, M. Moll ^a, R. Montero ^d, F.R. Palomo ^e, I. Vila ^c, M. Wiehe ^{a,f}, C. Quintana ^c

^a CERN, Switzerland

^b TU Dortmund University, Germany

^c Instituto de Física de Cantabria (CSIC-UC), Spain

^d Universidad del País Vasco, Spain

^e Universidad de Sevilla, Spain

^f Albert-Ludwigs-Universität, Germany

ARTICLE INFO

Keywords:

Two Photon Absorption-Transient Current

Technique

Low Gain Avalanche Detector

Gain reduction

Solid state detectors

ABSTRACT

The Low Gain Avalanche Detector (LGAD) technology is very promising for silicon timing detectors and currently heavily researched. Recent studies show that the gain of LGADs highly depends on the charge carrier density inside the gain layer. To study the charge carrier density related gain reduction, the Two Photon Absorption-Transient Current Technique (TPA-TCT) was employed to obtain information on the drift velocity and electric field of a LGAD for different charge carrier densities. The TPA-TCT uses fs-pulse infrared lasers to provide a three-dimensional resolution to study bulk effects. A compact TPA-TCT setup was developed at CERN and is used to measure current transients against the device depth of a 285 μm thick PIN and LGAD, fabricated by IMB-CNM. Methods to extract information about the electric field are employed to verify the charge carrier density related gain reduction. The gain layer of the LGAD is spatially resolved for the first time.

1. Introduction

Compared to standard PIN diodes, LGADs have an additional p^+ -layer implanted below the top n^{++} -electrode, which introduces a high electric field at the top junction and enables a gain [1]. The gain is driven by impact ionisation, which is sensitive to various operational parameters as e.g. the temperature [2], the bias voltage, and the excess charge carrier density [3]. This paper is focused on the latter parameter. When excess electrons (or holes) drift through the multiplication layer, they are multiplied and build up a temporal electric field with the holes and electrons from the multiplication process. The emerging additional electric field is counter directed towards the LGAD's electric field and reduces it. Therefore, the impact ionisation coefficient, i.e., the gain is reduced for the following electrons. The effect is non-destructive and reversible. It gets more pronounced for increasing charge carrier densities and increasing gain, i.e., increasing bias voltage, potentially leading to a significant drop in the gain. It is important to the LGAD technology, because a decreased gain leads to a reduced time resolution [3]. The Two Photon Absorption-Transient Current Technique (TPA-TCT) is, due to its three dimensional resolution and generation of

an adaptable charge carrier density, an ideal tool to study charge carrier density related effects along the device depth. Femtosecond pulse lasers with wavelengths in the non-linear absorption regime of silicon are used to generate charge only in a small volume around the laser's focal point [4,5].

2. Measurements

The TPA-TCT setup at CERN uses a 430 fs pulse fibre laser with a central wavelength of 1550 nm. For the here presented measurements the repetition rate is set to 200 Hz and an objective with a numerical aperture of 0.5 is used. The achieved beam waist is 1.3 μm and the Rayleigh length inside silicon is 12.5 μm . The setup and method is described in detail in the Refs. [5,6]. The measurements are performed on a LGAD and a PIN from IMB-CNM [7] run 8622 [8] from wafer 5. They are pristine silicon pad diodes with a physical thickness of 285 μm and no support wafer behind. Effects introduced by the multiplication layer are studied by comparing between the LGAD and the PIN detector. To investigate the charge carrier related gain reduction mechanism,

* Corresponding author at: CERN, Switzerland.

E-mail address: sebastian.pape@cern.ch (S. Pape).

in-depth scans with different laser intensities and bias voltages are performed. Higher laser intensities are used for the PIN to achieve an signal-to-noise ratio (SNR) that is comparable to the SNR in the LGAD measurements. These measurements are used to obtain information about the drift velocity and electric field in the devices. When the drift velocity is known, the electric field can be extracted from the known relation between the drift velocity and the electric field at a given bias voltage [9,10]:

$$v_{e,h} = \frac{\mu_{e,h}^0 E}{\left[1 + \left(\frac{\mu_{e,h}^0 E}{v_{e,h}^{\text{sat}}} \right)^{\beta_{e,h}} \right]^{1/\beta_{e,h}}}, \quad (1)$$

with the electric field E , the low field mobility $\mu_{e,h}^0$, the saturation drift velocity $v_{e,h}^{\text{sat}}$, and the parameter $\beta_{e,h}$ that describes the transition between the ohmic regime and the saturation velocity. The current, induced by the drifting charge carriers at the readout electrode of pristine PIN detectors is given by [11]:

$$I(t) = e_0 N_{e,h} (\vec{v}_e(t) + \vec{v}_h(t)) \vec{E}_w, \quad (2)$$

with the elementary charge e_0 , the amount of electron-hole pairs $N_{e,h}$, the drift velocity of the corresponding charge carrier $\vec{v}_{e,h}$, and the weighting field \vec{E}_w . Due to the three-dimensional charge carrier deposition of the TPA-TCT, the induced current is measured against the deposition depth $I(t, z)$. The prompt current method [12] is used to relate the induced current $I(t, z)$ to the drift velocity $v_{e,h}(z)$, by using the current induced after a short time after illumination t_{pc} , resulting in:

$$I(t = t_{pc} \approx 0, z) = \frac{e_0 N_{e,h}}{d} (v_e(t \approx 0, z) + v_h(t \approx 0, z)), \quad (3)$$

with the weighting field \hat{e}_z/d in a pad diode with thickness d . In the following, the current induced after $t_{pc} = 600$ ps is used as the prompt current.

3. Results

Prompt currents measured against the device depth in the PIN (a, b) and the LGAD (c, d), once measured with a low laser intensity and once with a higher laser intensity, are shown in Fig. 1. Three different bias voltages are used, whereby the PIN and the LGAD bias voltages are well above the full depletion voltage, which is reached at 32 V and 72 V, respectively. The PIN's bias voltages are chosen to yield approximately the same bulk fields as the LGAD's bias voltages, using:

$$V_{\text{bias,PIN}} \approx V_{\text{bias,LGAD}} \left(1 - \frac{d_{\text{GL}}}{d} \right) - V_{\text{GL}}, \quad (4)$$

with the bias voltage of the PIN $V_{\text{bias,PIN}}$, the bias voltage of the LGAD $V_{\text{bias,LGAD}}$, the thickness of the gain layer d_{GL} ($\approx 2 \mu\text{m}$), and the gain layer depletion voltage $V_{\text{GL}} = 32.2$ V. In the figures, the origin of the z -axis is set to the back side full width at half maximum (FWHM) of the drift velocity profile. Therefore, smaller z values correspond to the top side and greater z values to the back side of the DUT. To correct the z -axis for refraction inside silicon [5], the z values are multiplied with a correction factor: $z_{\text{Si}} = 3.754 \cdot z$. The data is normalised by the maximum prompt current to ease the qualitative comparison. For the PIN detector, the prompt current can be used, to extract the drift velocity profile against the device depth, after equation (3). The expected linear decrease of the prompt current, i.e., the drift velocity profile from the top towards the back side is found. This is related to a linear decreasing electric field inside the PIN. Furthermore, the drift velocity increases with an increasing bias voltage, as expected for the non-saturated regime. The prompt current profiles of the PIN are qualitatively the same for both intensities. The LGAD shows, compared to the PIN, a peak in the drift velocity profile at the top side ($z_{\text{Si}} \approx -0.28$ mm), which is related to the gain layer. Inside the gain layer, secondary charge carriers from the multiplication process also contribute to the

prompt current, which is the reason for the peak. The contribution of the secondary carriers to the prompt current becomes evident, when current transients from the top and back side are compared, as shown in Fig. 2. Fig. 2(a) shows current transients measured at the top and back side of the LGAD with the lower laser intensity and Fig. 2(b) shows the same current transients measured with the higher laser intensity. It can be seen that the primary carriers and secondary carriers are well separated for the current transients measured at the back side, and only primary carriers are present within the first 600 ps. At the top side the primary and secondary carriers cannot be easily distinguished and both contribute to the current during the first 600 ps. An overestimated drift velocity is extracted, if the peak's prompt current of the LGAD (Figs. 1(c) and 1(d)) is used, because the extraction of the drift velocity from the prompt current only works when the prompt current contains just the contribution from the primary carriers. Therefore, the prompt current method cannot be used to extract the drift velocity in the gain layer, but only in the bulk region. After the peak, the prompt current profiles also decreases linearly, due to the linear decreasing electric field in the bulk. The difference in height between the prompt current in the peak and the bulk indicates the presence of gain: the higher the difference, the higher the gain. The height difference decreases for an increasing laser intensity, i.e., increasing charge carrier density (compare Figs. 1(c) and 1(d)). This observation is linked to a reduced electric field, which lowers the gain, due to the charge carrier density related gain reduction [3].

The strong dependence of the gain on the bias voltage can be seen from the peak heights at different bias voltages. Furthermore, the peak width is much wider (FWHM $\approx 40 \mu\text{m}$) than expected from TCAD simulations ($< 5 \mu\text{m}$). This has two reasons, which are discussed in the following. First, the probing method can spread out small features. The resolution of TPA-TCT is given by the convolution of the probed structure with the laser's probing volume. If a structure is smaller or in the same order of size as the probing volume, the dimensions of this structure are not properly reproduced and features as peaks can appear spread out. Second, the time used for the prompt current t_{pc} is too long to measure the drift velocity localised enough. During the used $t_{pc} = 600$ ps, electrons with a saturated velocity can drift more than $60 \mu\text{m}$ [13]. Wherefore, the prompt current method only gives an averaged drift velocity over a certain spatial spread. If the charge carriers are deposited close towards the gain layer, the chosen t_{pc} can be long enough that even secondary charge carriers from the multiplication process contribute to the prompt current, which leads to an overestimation of such prompt currents, increasing the peak's width. The effect can be decreased for shorter prompt current times t_{pc} . However, shorter t_{pc} decrease the SNR. Nevertheless, this is the first time the electric field peak of the multiplication layer is resolved spatially, which is only possible because a sufficient SNR for low enough laser intensities is achieved.

Behind the DUT's surface ($z_{\text{Si}} > -0.015$ mm), signal is generated by the laser's reflection at the back side silicon-air interface [6]. For the PIN, the drift velocity measured behind the back side should mirror the drift velocity in front of the back side. However, a much lower drift velocity is found, which is an artefact of the prompt current method. The prompt current depends on the signal amplitude and therefore the laser intensity. To extract the drift velocity independent of the signal height, the signals have to be normalised by the total collected charge beforehand. A method to mitigate the intensity dependence of the drift velocity is currently under investigation.

4. Conclusion

For the first time the peak of the prompt current inside the multiplication layer in a LGAD was successfully spatially resolved. As well for the first time, the TPA-TCT was employed to verify the charge carrier density related gain reduction in a LGAD. For this, prompt current profiles, measured at different laser intensities, were compared and for

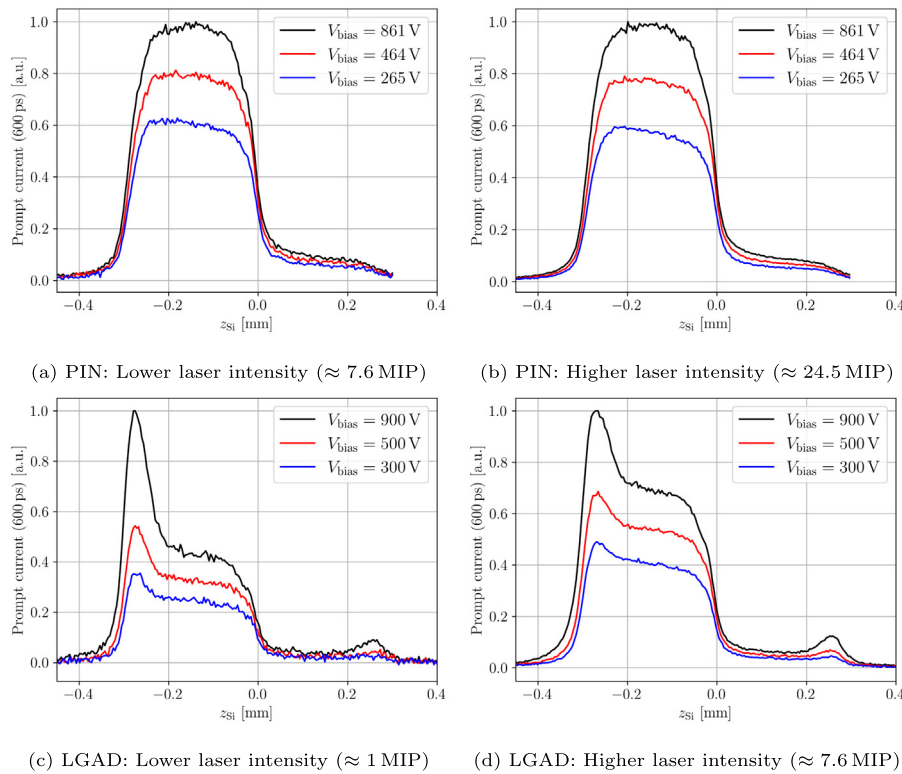


Fig. 1. Fig. (a) shows the prompt current profile of the PIN against the device depth for a lower laser intensity compared to the intensity used in the measurement shown in Fig. (b). Fig. (c) shows the prompt current profile of the LGAD against the device depth. Fig. (d) shows the same measurement, but measured with a higher laser intensity. For z_{Si} greater than ≈ -0.015 mm reflection from the back side interface is present. Same colours correspond to the same approximate bulk fields and the laser intensity is given in the equivalent charge a certain amount of minimum ionising particles (MIPs) deposit in a $300\mu\text{m}$ thick silicon PIN.

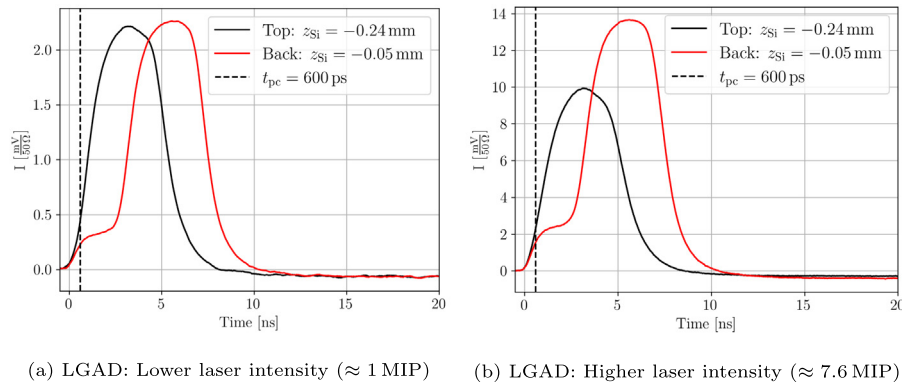


Fig. 2. Fig. (a) shows two current transients recorded at different device depth of the LGAD. The time used for the prompt current t_{pc} is indicated by the dotted line. Fig. (b) shows the same, but measured with a higher laser intensity. The bias voltage for both measurements is 900 V.

increasing charge carrier densities a decreasing gain, i.e., electric field was found. Besides, the intensity dependence of the prompt current method was observed and a method to avoid it was proposed. The application of such a method is currently under development.

Declaration of competing interest

The authors declare that they have no known competing financial interests or personal relationships that could have appeared to influence the work reported in this paper.

Acknowledgements

This project was performed within the framework of RD50 and has received funding from the European Union's Horizon 2020 Research

and Innovation programme under GA no 101004761 (AIDAinnova), the Wolfgang Gentner Program of the German Federal Ministry of Education and Research (grant no. 05E18CHA), the Spanish Ministry of Science (grant no. PID2020-113705RB-C31), and the CERN Knowledge Transfer Fund, through a grant awarded in 2017.

References

- [1] G. Pellegrini, et al., Technology developments and first measurements of low gain avalanche detectors (LGAD) for high energy physics applications, Nucl. Instrum. Methods Phys. Res. A 765 (2014) <http://dx.doi.org/10.1016/j.nima.2014.06.008>.
- [2] R. Mulargia, et al., Temperature dependence of the response of ultra fast silicon detectors, J. Instrum. 11 (2016) <http://dx.doi.org/10.1088/1748-0221/11/12/c12013>.
- [3] E. Currás, M. Fernández, M. Moll, Gain reduction mechanism observed in low gain avalanche diodes, Nucl. Instrum. Methods Phys. Res. A (2022) <http://dx.doi.org/10.1016/j.nima.2022.166530>.

- [4] M. Fernández García, et al., High resolution 3D characterization of silicon detectors using a two photon absorption transient current technique, Nucl. Instrum. Methods Phys. Res. A 958 (2020) <http://dx.doi.org/10.1016/j.nima.2019.162865>.
- [5] M. Wiehe, et al., Development of a tabletop setup for the transient current technique using two-photon absorption in silicon particle detectors, IEEE Trans. Nucl. Sci. 68 (2021) <http://dx.doi.org/10.1109/TNS.2020.3044489>.
- [6] S. Pape, et al., Characterisation of irradiated and non-irradiated silicon sensors with a table-top two photon absorption TCT system, in: Proceedings of the 12th International Conference on Position Sensitive Detectors, PSD12, 2021.
- [7] Centre Nacional de Microelectrònica, IMP-CNM-CSIC, Barcelona, Spain, 2018.
- [8] M. Wiehe, et al., Study of the radiation-induced damage mechanism in proton irradiated low gain avalanche detectors and its thermal annealing dependence, Nucl. Instrum. Methods Phys. Res. A 986 (2021) <http://dx.doi.org/10.1016/j.nima.2020.164814>.
- [9] D. Caughey, R. Thomas, Carrier mobilities in silicon empirically related to doping and field, Proc. IEEE 55 (1967) <http://dx.doi.org/10.1109/PROC.1967.6123>.
- [10] C. Jacoboni, et al., A review of some charge transport properties of silicon, Solid-State Electron. 20 (1977) [http://dx.doi.org/10.1016/0038-1101\(77\)90054-5](http://dx.doi.org/10.1016/0038-1101(77)90054-5).
- [11] S. Ramo, Currents induced by electron motion, Proc. IRE 27 (1939) <http://dx.doi.org/10.1109/JRPROC.1939.228757>.
- [12] G. Kramberger, et al., Investigation of irradiated silicon detectors by edge-TCT, IEEE Trans. Nucl. Sci. 57 (2010) <http://dx.doi.org/10.1109/TNS.2010.2051957>.
- [13] J. Becker, E. Fretwurst, R. Klanner, Measurements of charge carrier mobilities and drift velocity saturation in bulk silicon of 111 and 100 crystal orientation at high electric fields, Solid-State Electron. 56 (2011) <http://dx.doi.org/10.1016/j.sse.2010.10.009>.